Intermetallics 19 (2011) 1705–1710

Contents lists available at ScienceDirect

Intermetallics

journal homepage: www.elsevier.com/locate/intermet

Phase evolution and properties of $Ni_{50}Co_{23}Fe_2Ga_{25}$ Heusler alloy undercooled by electromagnetic levitation

R.V.S. Prasad, G. Phanikumar*

Department of Metallurgical and Materials Engineering, Indian Institute of Technology Madras, Chennai 600036, India

ARTICLE INFO

Article history:
Received 15 April 2011
Received in revised form
12 July 2011
Accepted 13 July 2011
Available online 12 August 2011

Keywords:
B. Phase identification
C. Rapid solidification processing
D. Microstructure
E. Phase stability
F. Electron microscopy
transmission

ABSTRACT

Microstructure and properties of bulk samples of $Ni_{50}Co_{23}Fe_2Ga_{25}$ Heusler alloy undercooled and solidified in an electromagnetic levitation facility have been studied. Microstructure characterization showed the samples to consist of a mixture of fcc phase and non-modulated tetragonal martensite phase at low undercoolings and a single phase microstructure containing only martensite at high undercooling. The fcc phase content increases with undercooling up to 170 K and then disappears at undercooling above 200 K. Hardness and magnetization correlate differently with the phase content of the sample.

1. Introduction

Ferromagnetic shape memory alloys such as a Ni_2MnGa are a new class of materials that have attracted the attention of research community [1]. These alloys suffer from poor ductility, high cost and processing difficulties such as loss of manganese. There is a growing interest in research to explore addition of a fourth element to the ternary Ni-based Heusler alloys that could improve ductility by forming a secondary ductile phase [2,3]. Several alternatives to the Ni–Mn–Ga system are also being explored [4]. Phase equilibria and magnetic properties of ternary alloys based on Ni–Mn–Ga with nickel and manganese replaced by iron and cobalt are being studied. Apart from Ni_2MnGa, there are many nickel containing ferromagnetic shape memory alloys such as Ni–Fe–Ga [5,6], Co–Ni–Ga [7–9] and Ni–Co–Mn–Ga [10] with an ordered B2-type or $L2_1$ phase exhibiting martensite transformation. These studies have shown that suitable selection of composition and heat treatment can lead to formation of fcc based (γ) phase that could improve ductility. Studies on $Ni_{49}Fe_{18}Ga_{27}Co_6$ have shown [11] that single crystals loaded in tension along [100] orientation exhibit a large temperature range of super elastic behavior. Most of these alloys exhibit giant magnetic field induced strain and are potential candidates for fabrication of magnetic shape memory (MSM) pumps, valves and actuators.

Electromagnetic levitation is a non-equilibrium solidification tool where undercooling of the alloy can be measured directly and rapid solidification could be achieved at relatively slow cooling rates [12]. The undercooling of the solidified alloy could be correlated to a number of microstructural changes such as grain refinement [13]], extended solid solubility and formation of metastable microstructures. Deep undercooling was shown to result in single phase microstructures in peritectic alloys such as Fe–Ge [14] and fine microstructure in Ni–Co–Ga alloys [13].

In the previous studies on alloys of composition close to Co_2NiGa, undercooling was shown to lead to subgrain formation and an increase in martensite transformation temperature [15,16]. Previous studies on $Ni_2(Fe,Co)Ga$ [17] with cobalt content of few at% have shown that the phase content, magnetic and martensitic transition temperatures are dependent on the composition of the alloy. Studies on undercooled samples of Ni_2CoGa using electromagnetic levitation have not been reported in the open literature. Experimentally measured ternary phase diagram of Co–Ni–Ga using diffusion experiments [7] showed that the phase-field of B2 phase (β) is wide and spans across the complete solid solution between nickel and cobalt for gallium contents above 35 at%. The two phase region of fcc and B2 phases is noted to be narrower for nickel rich compositions as seen in isothermal sections at 700 °C

* Corresponding author. Tel.: +91 44 2257 4770; fax: +91 44 2257 4752.
E-mail address: gphani@iitm.ac.in (G. Phanikumar).

0966-9795/$ – see front matter © 2011 Elsevier Ltd. All rights reserved.
doi:10.1016/j.intermet.2011.07.009

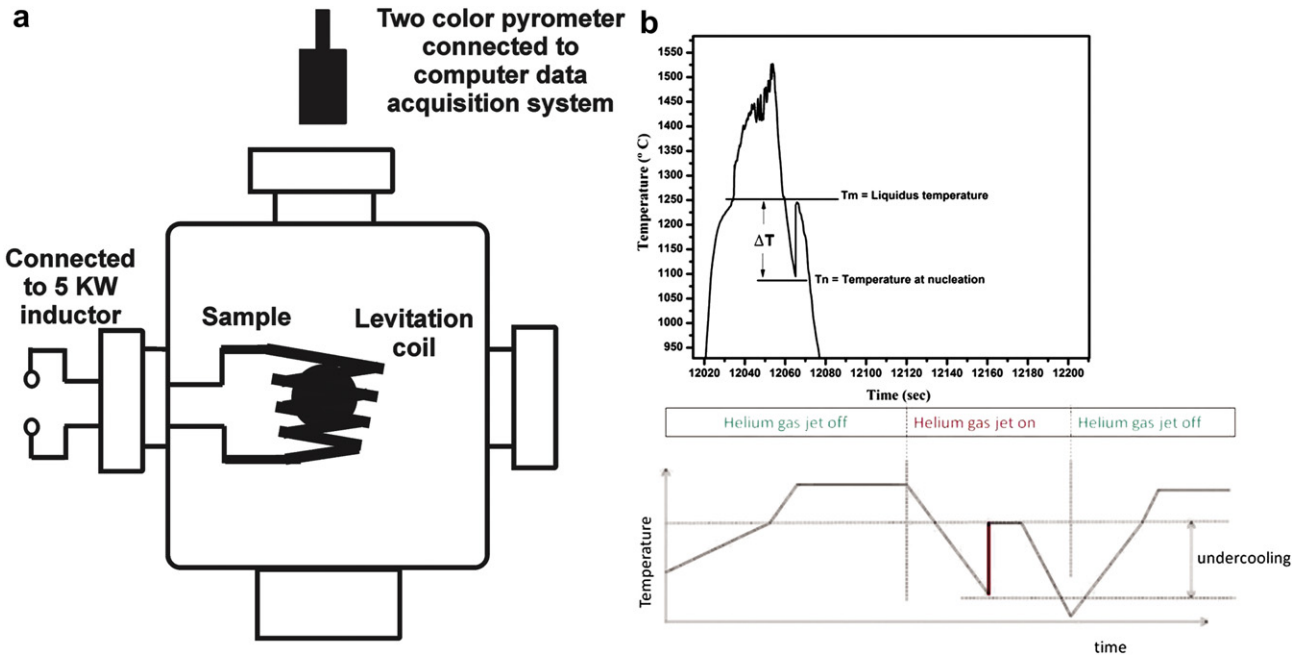

Fig. 1. (a) Schematic of electromagnetic levitation setup. (b) Typical thermal cycle during undercooling experiment in Electromagnetic levitation setup. Actual thermal profile for an undercooling of 170 K is shown in the inset.

and 1000 °C (Figs. 3 and 4 of Ref. [7]). In this study, an alloy close to Ni_2CoGa is chosen for study as it is likely to result in single phase β for deeply undercooled samples. Minor alloying with iron, based on previous trials [18,19] and studies on similar alloy systems [20] was explored to improve magnetic properties. In the present investigation, the composition chosen for study is $Ni_{50}Co_{23}Fe_2Ga_{25}$ Heusler alloy. The iron content chosen was small enough to form solid solution with the existing phases of Ni_2CoGa system and to preclude any new phase formation.

2. Experiments

$Ni_{50}Co_{23}Fe_2Ga_{25}$ alloy was prepared by arc melting of 99.99% pure nickel, cobalt, iron and gallium. The arc melting unit was evacuated to a pressure of 10^{-5}mbar and then backfilled with 99.99% argon. Samples in the form of buttons weighing around 0.8 g and diameter around 6–8 mm were prepared in the arc melting unit and melted four times to ensure homogeneity of the composition. The sample preparation was identical for all the samples.

The experiments were performed in an electromagnetic levitation facility. A schematic of the setup is shown in Fig. 1a. Each sample was inserted into the levitation coil supported by an alumina sample holder. The levitation chamber was evacuated to 10^{-6} mbar and subsequently backfilled with 99.99% pure argon gas. Once the sample was levitated, the alumina sample holder was withdrawn. An infrared two-color pyrometer coupled with a computer recorded the thermal cycles of the levitated droplet with ±5 K accuracy and at a sampling rate of 100 Hz. A typical thermal cycle is shown in Fig. 1b. The sample is levitated and allowed to reach a temperature well above the liquidus (say 150–200 K above T_m) of the particular alloy system by RF induction heating. Cooling portion of the thermal cycle is achieved by blowing 99.99% pure helium gas through a set of nozzles onto the sample. During cooling cycle, the solidification of undercooled sample initiates at the nucleation temperature denoted by a sudden

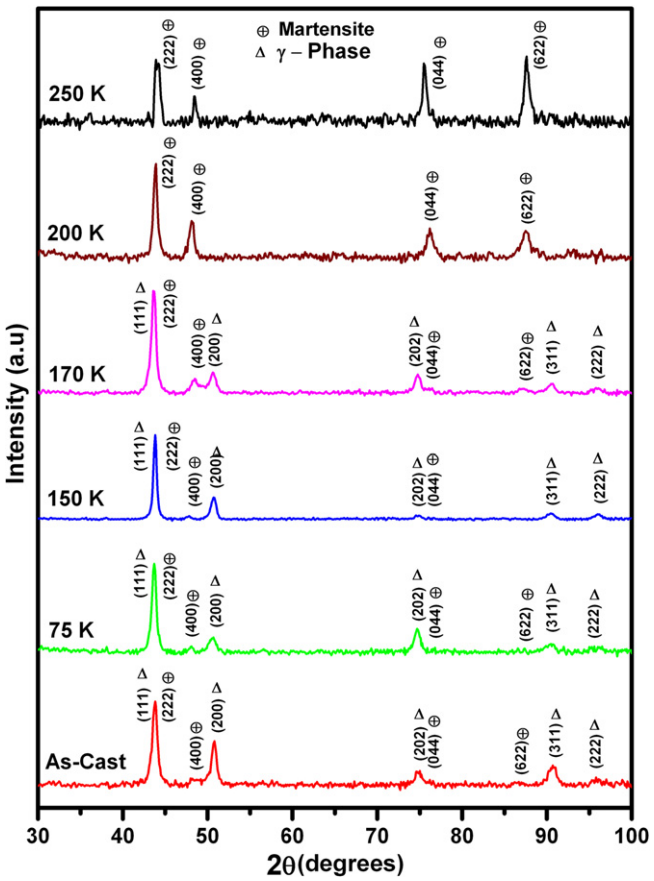

Fig. 2. XRD patterns for the $Ni_{50}Co_{23}Fe_2Ga_{25}$ alloy for samples in as-cast and solidified after different undercooling.

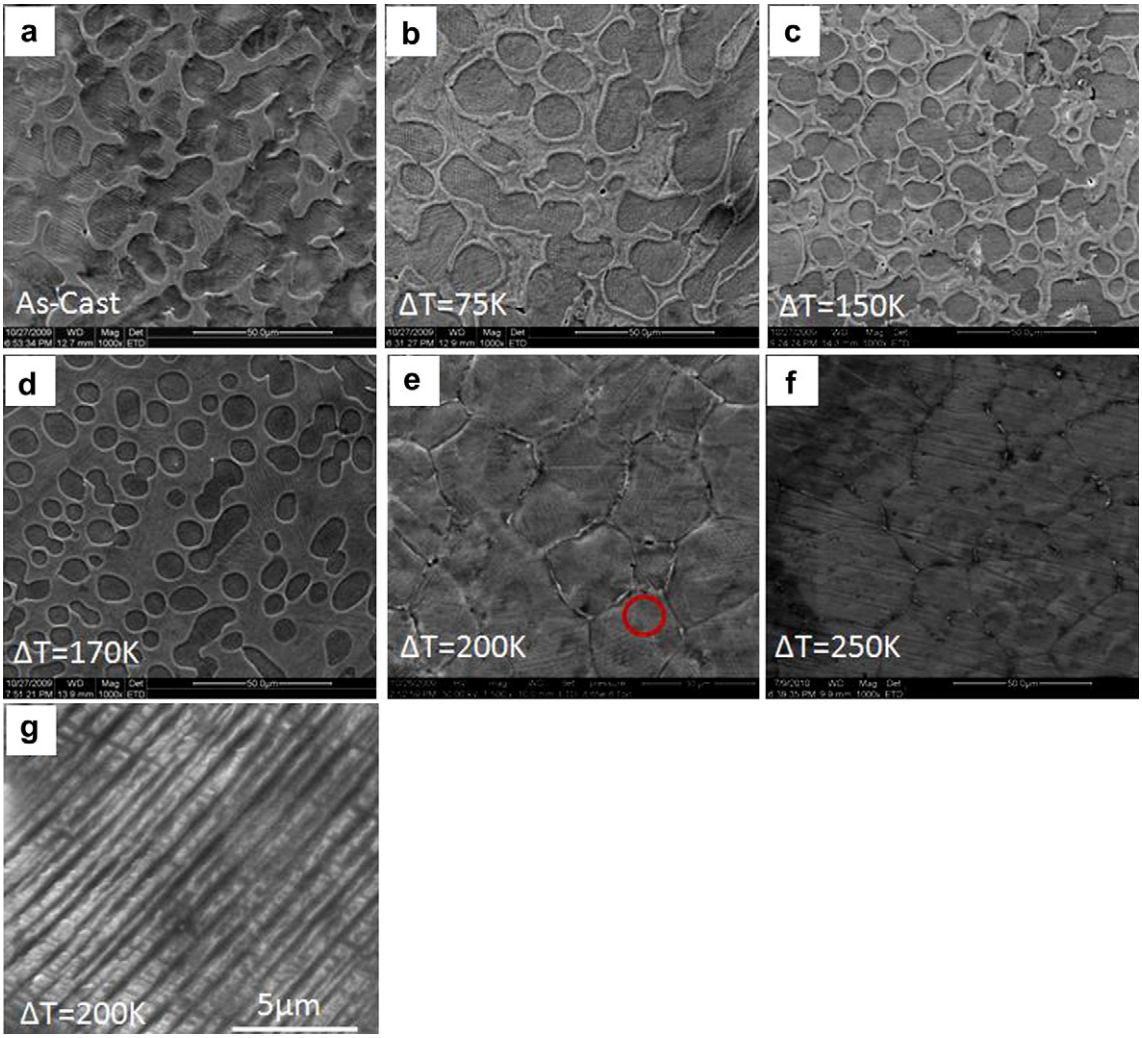

Fig. 3. Secondary electron images of samples in different conditions: (a) as-cast and solidified after undercooling of (b) 75 K (c) 150 K (d) 170 K (e) 200 K and (f) 250 K (g) sampled undercooled to 200 K at higher magnification showing martensite twins.

rise in the thermal signal (recalescence). The difference between the nucleation temperature (T_n) and the liquidus (T_m) is taken as bulk undercooling. As an illustration, an actual thermal cycle of sample taken out after 170 K undercooling is shown in the inset of Fig. 1b.

During each experiment of levitation, the samples undergo several thermal cycles that correspond to different levels of undercooling. The final thermal cycle determines the undercooling of the sample taken out after solidification for microstructure characterization. Extended duration of levitation at temperatures significantly higher than the liquidus could lead to preferential loss of elements. Hence, the number of thermal cycles and the duration of levitation were kept roughly same for all samples. Composition of all the levitated and solidified samples was measured by the EDS attachment to SEM and ensured to remain at the nominally chosen one. Surface oxidation was not noticeable. In this study, samples taken out after solidification at undercooling between 75 K and 250 K are studied. All the samples were characterized using transmission electron microscopy and scanning electron microscopy. Phase identification and structural characterization was performed by X-ray diffraction with Cu-Kα radiation. Magnetic characterization studies were performed using a vibrating sample magnetometer.

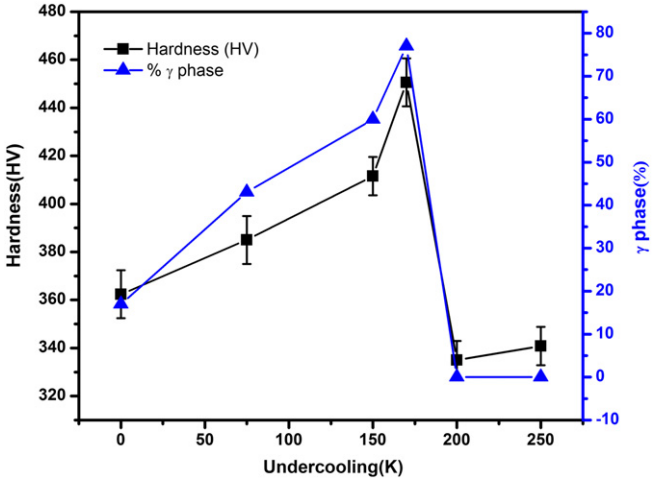

Fig. 4. Plot of fcc (γ) phase fraction and vickers hardness at 100 g load for samples solidified after undercooling to different levels.

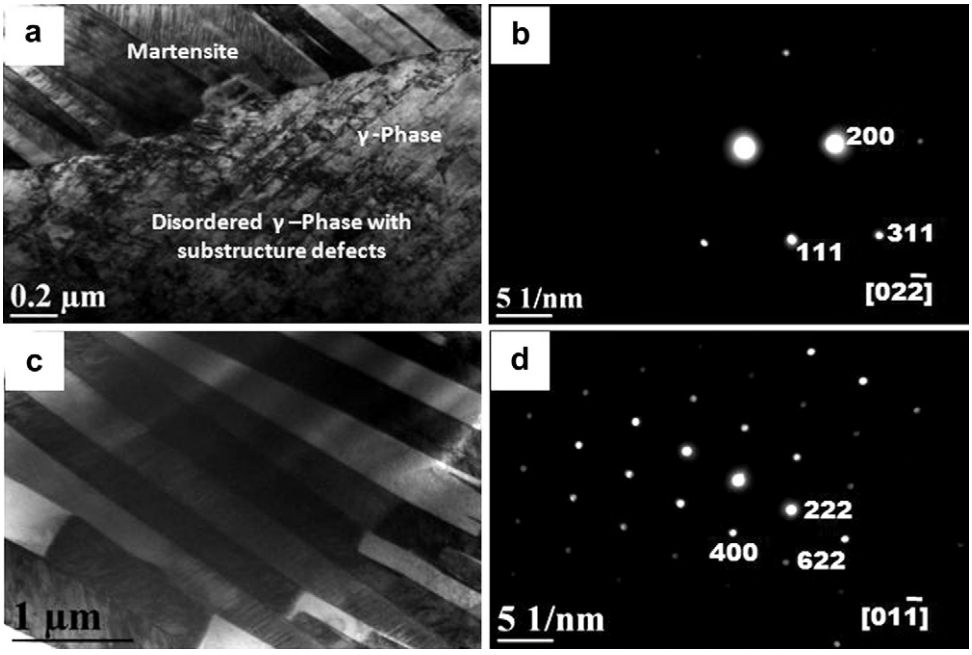

Fig. 5. TEM analysis of alloy solidified after an undercooling of 170 K: (a) Bright field image showing mixture of martensite phase and γ phase (b) SAED pattern taken from γ phase region indexed to F.C.C along [02$\bar{2}$] zone axis (c) Bright field image showing martensite phase (d) SAED pattern taken from martensite phase indexed to non-modulated tetragonal structure along [01$\bar{1}$] zone axis.

3. Experimental results

XRD patterns of samples solidified at different levels of undercooling are plotted in Fig. 2. The arc melted (as-cast) sample exhibits a two phase mixture corresponds to both γ phase (referred to as fcc phase henceforth) and non-modulated tetragonal martensite. Samples of low undercooling (up to about 170 K) consist of two phase mixture of fcc phase and non-modulated tetragonal martensite. However, at high undercooling (above 200 K), the sample is single phase consisting of only martensite.

Secondary electron (SE) images of as-cast and levitated samples at different levels of undercooling are shown in Fig. 3. The as-cast sample exhibits phase mixture of both fcc phase and martensite. As the degree of undercooling (ΔT) increases from 75 K to 170 K, as shown in Fig. 3b–d, the fraction of fcc phase increases. Using an image analysis software, the amount of fcc phase is determined to be 17% for as-cast sample and it increases to 43% ($\Delta T = 75$ K), 62% ($\Delta T = 150$ K) and 77% ($\Delta T = 170$ K) for undercooled samples. The data is also plotted in Fig. 4. From the micrographs, it is evident that the fcc phase surrounds the martensite phase that is in a dendritic morphology. Samples solidified at an undercooling of 200 K and above (250 K) consist of only martensite phase in equiaxed morphology (Fig. 3e and f). Martensite twins could be confirmed from images taken at higher magnification (Fig. 3g).

Vickers hardness using a load of 100 g was measured for all the samples. The indentation covers both the phases and is representative of the averaged hardness of the mixture of phases. The data averaged for 10 indentations for each sample are plotted in Fig. 4. The average hardness value increases from 362 to 450 $HV_{100\ g}$ in proportion to the fraction of fcc phase/degree of undercooling. However, samples solidified at high undercooling (>200 K) exhibit significantly lower hardness between 335 and 340 $HV_{100\ gm}$.

Detailed transmission electron microscopy (TEM) was used to study the microstructures of all the samples (Figs. 5 and 6). The crystal structures of the phases were confirmed using the selected area electron diffraction (SAED) pattern. The fcc phase can be noticed to be consisting of dislocation networks. The as-cast sample consists of a phase mixture of γ phase of fcc structure and martensite phase of non-modulated tetragonal structure, respectively.

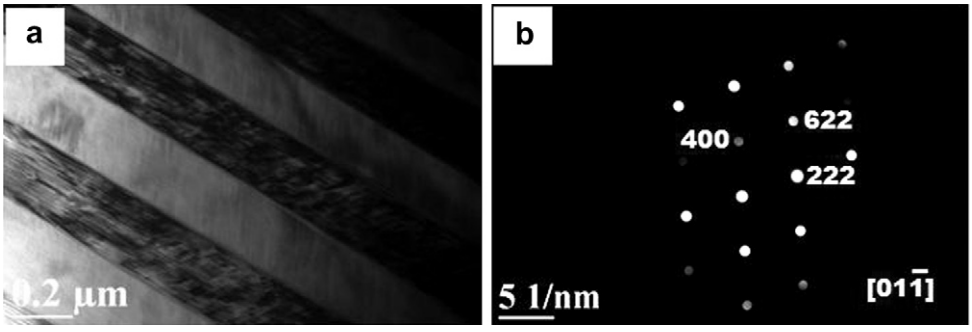

Fig. 6. TEM analysis of sample solidified after undercooling of 200 K: (a) bright field image showing martensite phase (b) SAED pattern taken from martensite phase indexed to non-modulated tetragonal structure along [01$\bar{1}$] zone axis.

Samples solidified at low (<200 K) undercooling exhibited a phase mixture similar to as-cast samples. As an illustration, the microscopy analysis of a sample solidified at an undercooling of 170 K is shown in Fig. 5. The bright field image in Fig. 5a shows the martensite phase and the fcc phase consisting of dislocation networks. The SAED pattern taken with $[02\bar{2}]$ zone axis from the disordered region confirms the fcc phase. The bright field image and SAED pattern taken with the $[01\bar{1}]$ zone axis from the martensite region are shown in Fig. 5c and d, respectively.

Samples solidified at high undercooling (>200 K) exhibited a single phase microstructure consisting of only martensite. The bright field image (Fig. 6a) confirms martensite phase. The SAED pattern (Fig. 6b) taken by using $[01\bar{1}]$ zone axis confirms the non-modulated tetragonal structure of martensite.

A survey of composition analysis using EDS attached to SEM was performed on the two phases in all the samples solidified at different undercooling. The data (not shown here for brevity) indicates that there is a partitioning of elements in the following manner. The fcc phase contained less iron (lowest : 1.4 at%) compared to the martensite phase (highest : 3.0 at%) in all the two phase microstructures. Similarly, gallium is found to partition in favor of the fcc phase (highest : 29 at%) compared to the martensite phase (17.8%). The as-solidified samples showed microsegregation in nickel and cobalt that exhibited no clear partitioning between the two phases at different locations in the sample.

Plots of magnetization (M) vs. magnetic field (H) measured for all the samples are shown in Fig. 7. These data indicate that as the degree of undercooling increases, the magnetization (emu/g) decreases up to 14 emu/g. However, at 200 K undercooling, the magnetization was recovered to higher value of 27 emu/g.

4. Discussion

Undercooling plays an important role in phase selection in peritectic systems [21]. A schematic vertical section of Ni–Co–Ga phase diagram (as shown in Fig. 2 of the study by Liu and co-workers [22]) exhibits a peritectic reaction ($L+\gamma \rightarrow \beta$) for alloys near Co_2NiGa. From the ternary phase diagram information available for the Ni–Co–Ga system from experimental studies in open literature [7], one can say that the composition chosen falls in the two phase region (fcc + β) of the ternary phase diagram.

During solidification of undercooled melts, the primary phase solidifies in dendrite morphology due to negative thermal gradient ahead of the solid–liquid interface. The secondary phase could then solidify from the inter-dendritic liquid or by a reaction between the primary phase and the liquid phase. The morphology of the martensite phase$\beta(m)$ is in the form of dendrites in all the samples solidified at lower (<200 K) undercooling. This indicates that the primary phase to solidify for these alloys is likely to be β phase (austenite/ordered $B2/L2_1$ phase).

The possibility that γ phase is the primary phase and that the solidification is through a peritectic reaction is less likely for the following reason. During the peritectic reaction, the peritectic phase would usually nucleate at the interface of the primary phase and the liquid and would grow at the expense of the parent phases. Incomplete peritectic reactions would be indicated by the presence of primary phase at the core of the dendrite morphologies [14]. Absence of either the γ phase at the core of dendrite morphologies or any signature features of a peritectic reaction in the microstructure imply that the β phase is likely to be the primary phase. However, a direct disambiguation of this issue could be addressed by in-situ X-ray diffraction studies using synchrotron radiation.

Earlier studies on undercooling of Co_2NiGa alloys showed only a refinement of γ phase and single phase microstructures were not reported even at an undercooling of 230 K [13]. In this study on alloys close to the stoichiometry of Ni_2CoGa, samples solidified at higher (>200 K) undercooling consist of only martensite. Single phase microstructures in samples solidified after high undercooling show that the primary phase β (appearing in sample at room temperature as $\beta(m)$), is in equiaxed morphology indicating grain refinement. The authors believe that this observation could be useful while assessing the thermodynamic data for this system.

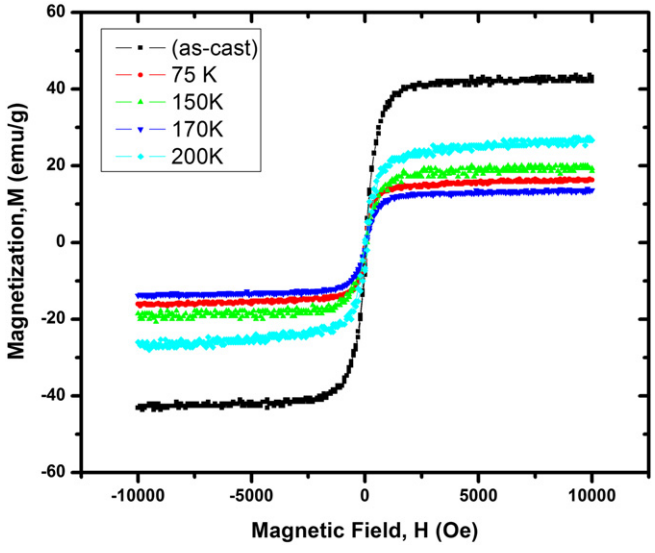

Fig. 7. Magnetization vs. Magnetic field plots for samples solidified at different degree of undercooling.

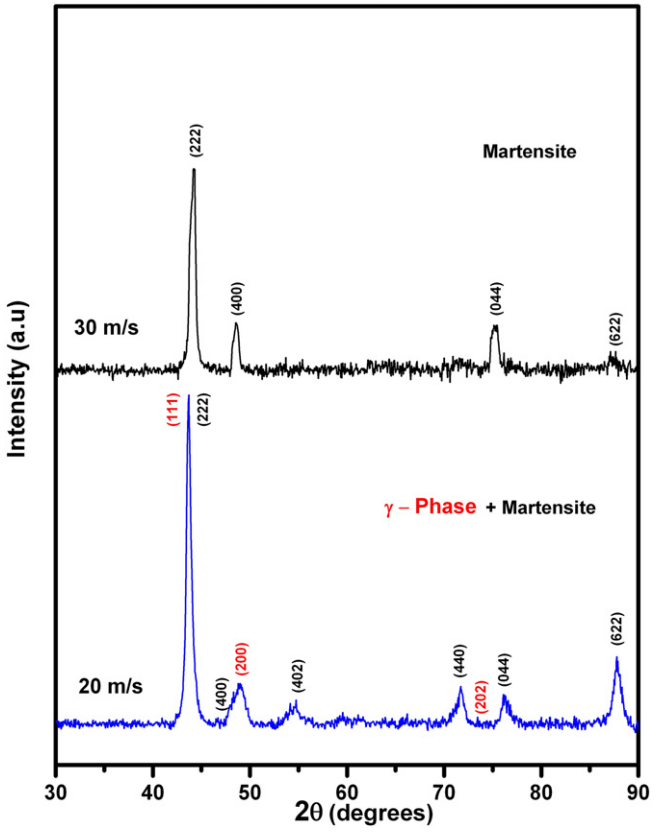

Fig. 8. XRD patterns of melt-spun ribbons of $Ni_{50}Co_{23}Fe_2Ga_{25}$ alloy at high speed (30 m/s, above) and low speed (20 m/s, below).

Based on the microstructures observed, one can propose that the likely sequence of solidification for lower undercooling is $L \rightarrow L+\beta \rightarrow \gamma+\beta \rightarrow \gamma+\beta(m)$. The sequence modifies to the following for higher undercooling: $L \rightarrow \beta \rightarrow \beta(m)$.

The length scale and morphology of the γ phase changes as the degree of undercooling increases up to 170 K. At higher undercooling, the growth rate of the dendrite is higher and the dendrite tip radius smaller [12]. Thus, in an undercooled and solidified sample, a smaller area fraction of the primary phase at higher undercooling is expected. Ma and co-workers [[23]] reported that γ phase could impede the propagation of brittle crack in ferromagnetic shape memory alloys and thus contributes to the enhancement of toughness. They also showed that uniform distribution of γ phase in the martensite matrix could lead to composite nature of these materials. Microstructures of the as-cast $Ni_{50}Co_{23}Fe_2Ga_{25}$ alloy show that the γ phase is randomly distributed. However, as the undercooling increases to 170 K, the morphology becomes more uniform and at the same time the volume fraction of γ phase increases to 77%. Zheng and co-workers [24] have reported similar observations on Ni–Fe–Ga alloy.

Hardness values show that the increase can be attributed to the volume fraction of fcc phase. Structure defects and antisite defects are known to cause hardening in Heusler alloys, particularly for compositions away from the stoichiometric ones [25]. Higher hardness of the sample at higher undercooling could also be due to higher defect concentration in the fcc phase. Bright field images (such as Fig. 5a) also corroborate the argument.

Magnetization of $Ni_{50}Co_{23}Fe_2Ga_{25}$ alloys is due to the $\beta(m)$ phase. Thus, there is a decrease of magnetization with increasing undercooling and the recovery to the highest value of 27 emu/g in single phase samples solidified at undercooling of 200 K. This demonstrates that the microstructure and phase fractions are important in determining the magnetic properties of the alloy.

Kurz and Gilgien have demonstrated in Al–Cu system that solidification microstructures obtained from techniques that employ different velocities and thermal gradients could be connected by a microstructure map using interface response functions [26]. Such a detailed study on a ternary system such as Heusler alloys is a challenge. However, melt-spinning of $Ni_{50}Co_{23}Fe_2Ga_{25}$ alloy at different speeds showed a correlation highlighting the importance of microstructure maps. Ribbon samples melt-spun at low speed (20 m/s) consist of a mixture of fcc and martensite phases whereas those melt-spun at high speed (30 m/s) consist of single phase microstructure of only martensite (Fig. 8). Details of the melt-spinning technique and the optimization of wheel speeds are not given here for brevity and are similar to those in earlier published work [18,19]. It is interesting to note that higher wheel speeds that are supposed to lead to higher undercooling of the melt have led to phase content similar to deeply undercooled samples. This comparison of two techniques that have different thermal gradients in the melt is preliminary. However, the results promise that the phase selection in this alloy system is applicable to multiple processing techniques.

5. Summary and conclusions

$Ni_{50}Co_{23}Fe_2Ga_{25}$Heusler alloy has been processed by electromagnetic levitation technique. The samples solidified at low undercooling consist of fcc phase and non-modulated tetragonal phase. At high undercooling (>200 K), the samples are single phase and consist of only martensite. Hardness is proportional to the fraction of fcc phase in the sample. Saturation magnetization is inversely proportional to the fraction of fcc phase in the sample. Studies showed that microstructures and thus the properties correlate with undercooling.

Acknowledgments

One of the authors (GP) gratefully acknowledges financial support from Indian Space Research Organization for financial support in setting up the national electromagnetic levitation facility at IIT Madras. The authors thank Dr. M. Manivel Raja, Advanced Magnetics Group, Defense Metallurgical Laboratory, Hyderabad for magnetic measurements and useful discussions.

References

[1] Ullakko K, Huang JK, Kantner C, Kokorin VV, O'Handley RC. Applied Physics Letters 1996;69:1966–8.
[2] Wang HB, Chen F, Gao ZY, Cai W, Zhao LC. Materials Science and Engineering A 2006;438–440:990–3.
[3] Soto D, Hernández Francisco Alvarado, Krenke Thorsten, Flores-Zúñiga Horacio, Moya Xavier, Mañosa Lluís, et al. Physical Review B 2008;77:184103.
[4] Pons J, Cesari E, Segui C, Masdeu F, Santamarta R. Materials Science and Engineering A 2008;A481-482:57–65.
[5] Oikawa K, Omori T, Sutou T, Morito H, Kainuma R, Ishida K. Metallurgical and Materials Transactions A 2007;38A:767–76.
[6] Omori T, Kamiya N, Sutou Y, Oikawa K, Kainuma R, Ishida K. Materials Science and Engineering A 2004;378:403–8.
[7] Ducher R, Kainuma R, Ishida K. Journal of Alloys and Compounds 2008;466:208–13.
[8] Oikawa K, Ota K, Imano Y, Omori T, Kainuma R, Ishida K. Journal of Phase Equilibria and Diffusion 2006;27:75–82.
[9] Liu J, Xia Mingxu, Huang Yanlu, Zheng Hongxing, Li. Jianguo. Journal of Alloys and Compounds 2006;417:96–9.
[10] Segui C, Cesari E. Intermetallics 2011;19:721–5.
[11] Panchenko E, Chumlyakov Y, Maier HJ, Timofeeva E, Karaman I. Intermetallics 2011;18:2458–63.
[12] Herlach DM. Materials Science and Engineering 1994;R12:177–272.
[13] Li JZ, Liu J, Zhang MX, Li JG. Refinement of the γ phase with melt undercooling in a two-phase Co_2NiGa magnetic shape memory alloy. Journal of Alloys and Compounds 2010;499:39–42.
[14] Phanikumar G, Biswas Krishanu, Funke Oliver, Holland-Moritz Dirk, Herlach Dieter M, Chattopadhyay K. Acta Materialia 2005;53:3591–600.
[15] Li J, Li J. Journal of Alloys and Compounds 2011;509:4242–6.
[16] Li J, Li J. Journal of Alloys and Compounds 2011;509:1563–6.
[17] Liu J, Scheerbaum Nils, Hinz Dietrich, Gutfleisch Oliver. Acta Materialia 2008;56:3177–86.
[18] Prasad RVS, Phanikumar G. Journal of Material Science 2009;44:2553–9.
[19] Prasad RVS, Phanikumar G. Materials Science Forum 2010;649:35–40.
[20] Wu Zhigang, Liu Zhuhong, Yang Hong, Liu Yinong, Wu Guangheng, Woodward Robert C. Intermetallics 2011;19:445–52.
[21] Umeda T, Okane T, Kurz W. Acta Materialia 1996;44:4209–16.
[22] Liu J, Xia M, Huang Y, Zheng H, Li J. Journal of Alloys and Compounds 2006;417:96–9.
[23] Ma Y, Yang Shuiyuan, Liu Yong, Liu Xingjun. Acta Materialia 2009;57:3232–41.
[24] Zheng HX, Xia MX, Liu J, Li JG. Journal of Alloys and Compounds 2005;388:172–6.
[25] Hosoda H, Wakashima K, Sugimoto T, Miyazaki S. Materials Transactions of the Japan Institute of Metals 2002;43:852–5.
[26] Kurz W, Gilgien P. Material Science and Engineering A 1994;A178:171–8.